Int. J. Electrochem. Sci., 10 **(2015)** 5548 - 5560

International Journal of
ELECTROCHEMICAL
SCIENCE
www.electrochemsci.org

Biomimetic Olfactory Sensor for Dynamically and Conveniently Monitoring Ligands Binding to Odorant-Binding Proteins with Impedance Sensing

Yao Yao[1], *Yanli Lu*[1], *Qian Zhang*[1], *Diming Zhang*[1], *Shulin Zhuang*[2], *Hongliang Li*[3], *Jianzhen Shan*[4], *Qingjun Liu*[1,*]

[1] Biosensor National Special Laboratory, Key Laboratory for Biomedical Engineering of Education Ministry, Department of Biomedical Engineering, Zhejiang University, Hangzhou, 310027, P.R. China
[2] College of Environmental and Resource Sciences, Zhejiang University, Hangzhou, 310027, P.R. China
[3] College of Life Sciences, China Jiliang University, Hangzhou 310018, P.R. China
[4] Second Affiliated Hospital, School of Medicine, Zhejiang University, Hangzhou 310058, P.R. China
[*]E-mail: qjliu@zju.edu.cn

Received: 31 March 2015 / *Accepted:* 7 May 2015 / *Published:* 27 May 2015

In olfactory research, odorant-binding proteins (OBPs) are promising candidates for developing biomimetic systems. In this paper, we designed an impedance sensing system by utilizing OBPs of honeybee as sensing membrane to detect molecules. Its responses to odorants of isoamyl acetate and butanedione were recorded by impedance spectroscopy. The relative decrease of charge transfer resistance of the sensing concentration was optimized from 10^{-9} M to 10^{-4} M. Sensitivity and selectivity of the sensor were investigated from different proteins, ligands and electrodes. To explore molecular recognition processes of the olfactory sensor, the tertiary structure of OBPs was modeled and the odorants were docked into its special hydrophobic cavity. The correlations between the conformational changes of the protein and impedance spectrum changes of the biosensor were discussed with a theoretical mode. The results suggested that the OBPs-based olfactory sensor could dynamically detect the specific ligand-protein interactions. The biomimetic design that made full use of the conformational change properties could provide a sensitive, low-cost, real-time, label-free and ease of operating approach for chemicals detection. If needed, the approach could be applied to other proteins, which shows attractive potential for biotechnological applications.

Keywords: Biomimetic design, Olfactory biosensor, Odorant-binding protein, Dynamic monitoring, Electrochemical impedance spectroscopy

1. INTRODUCTION

As a very elaborate sense, olfactory system can detect an extremely wide variety of volatile molecules at very low concentrations. Since olfactory systems play important roles in recognizing environmental conditions, kinds of olfactory researches have been carried out due to their potential sensing applications. As one of the conventional biomimetic technologies, the electronic sensors could mimic animals' olfactory systems to detect odorants by their artificial materials [1]. The detection ability mainly depends on absorb ability or catalysis of those materials to special odorants. Although much progress has been made, these methods do not work as perfect as the biology olfactory systems in specificity and sensitivity [2-5].

The understanding of the biological olfactory system provides valuable insight into odor detection. For living organisms, the initial step in odors detection is the capture of the molecules by some extracellular proteins and membrane-bound olfactory receptors (ORs) [6-7]. As one kind of the major peripheral olfactory proteins, odorant-binding proteins (OBPs) are small, water-soluble proteins, highly expressed in the nasal mucus of vertebrates and sensillum lymph of insects [8-9]. OBPs provide the first filtering mechanism for chemical signals and mediate the activation of the ORs. Both OBPs and ORs contribute to the specificity of the cell response and lead to the remarkable selectivity of the olfactory system.

In olfactory biosensors researches, ORs have been commonly used sensing molecules [2-3]. However, ORs are G protein coupled receptors, which need to stay in the cellular membrane environment to maintain their functionality. Compared with membrane protein ORs, OBPs were easier to be isolated and purified [10-11]. At the same time, OBPs were robust enough to stand up to wide ranges of pH and temperatures for substantial mistreatments, without denaturing and losing their binding properties [12-14]. In addition, OBPs could be expressed in bacterial systems at low cost. All of these excellent properties suggest that OBPs possibly provide a new recognizing approach in the development of biomimetic systems.

In this study, an OBP of honeybees was separated and purified. An impedance sensing system was designed to study the protein-ligand interactions. With series of controlled experiments conducted, sensitivity and selectivity of the biomimetic olfactory sensor were investigated. To explore the essence of biological reaction, the tertiary structure of OBPs and ligand were simulated by molecular docking. In addition, an impedance model was established to discuss correlations between the change of protein conformation and electrical impedance. The docking results and modified model verified the validity of experiments. The biomimetic design could not only advance the progress in the understanding of the binding properties of OBPs, but also show attractive potentials for biotechnological applications.

2. EXPERIMENTAL METHODS

2.1. Biomimetic design

OBPs are promising candidates as biological elements for developing biomimetic sensors. The proteins have an internal binding cavity, which provided a valuable basis for the broad affinity and

specificity to a variety of hydrophobic odorants, such as pheromones and floral odorants [15-16]. This paper focused on Acer-ASP2 that was a kind of significant honeybee OBPs. Based on amino acid sequence of Acer-ASP2, the tertiary structure of Acer-ASP2 was modeled by I-TASSER server [17]. To predict the binding mode of ligand-protein interaction, the ligands were docked into the binding site of Acer-ASP2 using the Molegro Virtual Docker (MVD) Version 4.2 following default protocols. The binding pocket covers a site with a user-defined origin and a radius of 15 Å. Thereafter, a theoretical model was established to discuss the correlations between the conformational changes of the protein and impedance spectrum changes of the biosensor.

2.2. Proteins and odorants

The expression and purification of the active recombinant Acer-ASP2 were cloned from the full-length cDNA of adult worker bees [18]. Briefly, using reverse transcription-polymerase chain reaction (RT-PCR) and PET-30a (+)/BL21 (DE3) prokaryotic expression system, Acer-ASP2 from antenna of worker bees were cloned and expressed by transformed into *Escherichia coli* BL21 competent cells. After the bacterial cells harvested, the inclusion body of Acer-ASP2 was severely precipitated in 1.5 M urea in ddH_2O and finally freeze-dried. The protein was resuspended (500 μg/ml) in phosphate buffered saline (PBS, pH=7.4) and saved under 4 °C for the following experiments.

Isoamyl acetate (a typical alarm pheromone to the honeybee), which can specifically bind to Acer-ASP2, was chosen as the high-affinity ligand, while butanedione (a nonspecific ligand to the protein) was used as a representative of low-affinity ligand. Both of them were diluted to 10^{-9} M, 10^{-8} M, 10^{-7} M, 10^{-6} M, 10^{-5} M and 10^{-4} M with PBS. In addition, as one of the most common proteins, bovine serum albumin (BSA) was used as a negative protein to demonstrate the binding properties of OBPs. The BSA was dissolved in PBS at the same concentration with Acer-ASP2 (500 μg/ml). All other chemicals were of analytical grade and were purchased from Sigma-Aldrich (USA).

2.3. Electrode fabrication

Interdigitated electrodes, which have uniform electric fields and high electrode coverage, were used to measure odorants binding to Acer-ASP2 by real-time impedance detection. The fabrication of the electrode arrays using semiconductor technology (Fig. 1A). Briefly, a 4-inch sterilized Pyrex glass 7740 was chosen as the insulating substrate. After sputtering a layer of Cr (20 nm thick) on the glass, a layer of Au (200 nm thick) was sputtered with the same method. Subsequently, through conventional lithography and etching techniques, the interdigitated electrodes, interconnects and pads were patterned from this composited metallic layer. Afterwards, the sensing ship was packaged with PCB board (Fig. 1B). Perspex with eight pairs round holes was used as the impedance detecting well in the experiments. Finally, the perspex was adhered on the board with liquid adhesive, epoxy resin, when the round holes were aligned with the electrodes.

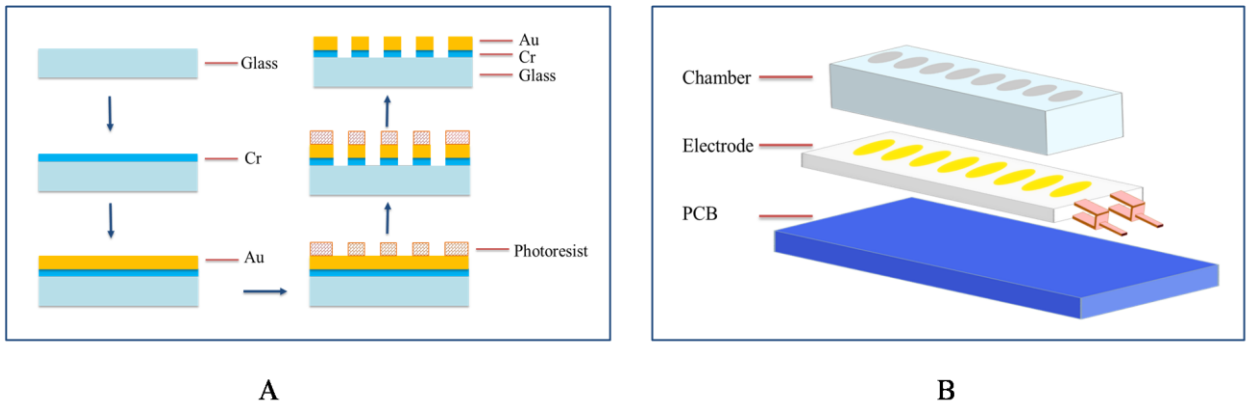

Figure 1. Electrodes and device of the olfactory sensor. (A) The fabrication process of interdigitated electrode arrays. (B) Schematic of device consisting of chamber, electrode, and PCB board.

2.4. Biomimetic system

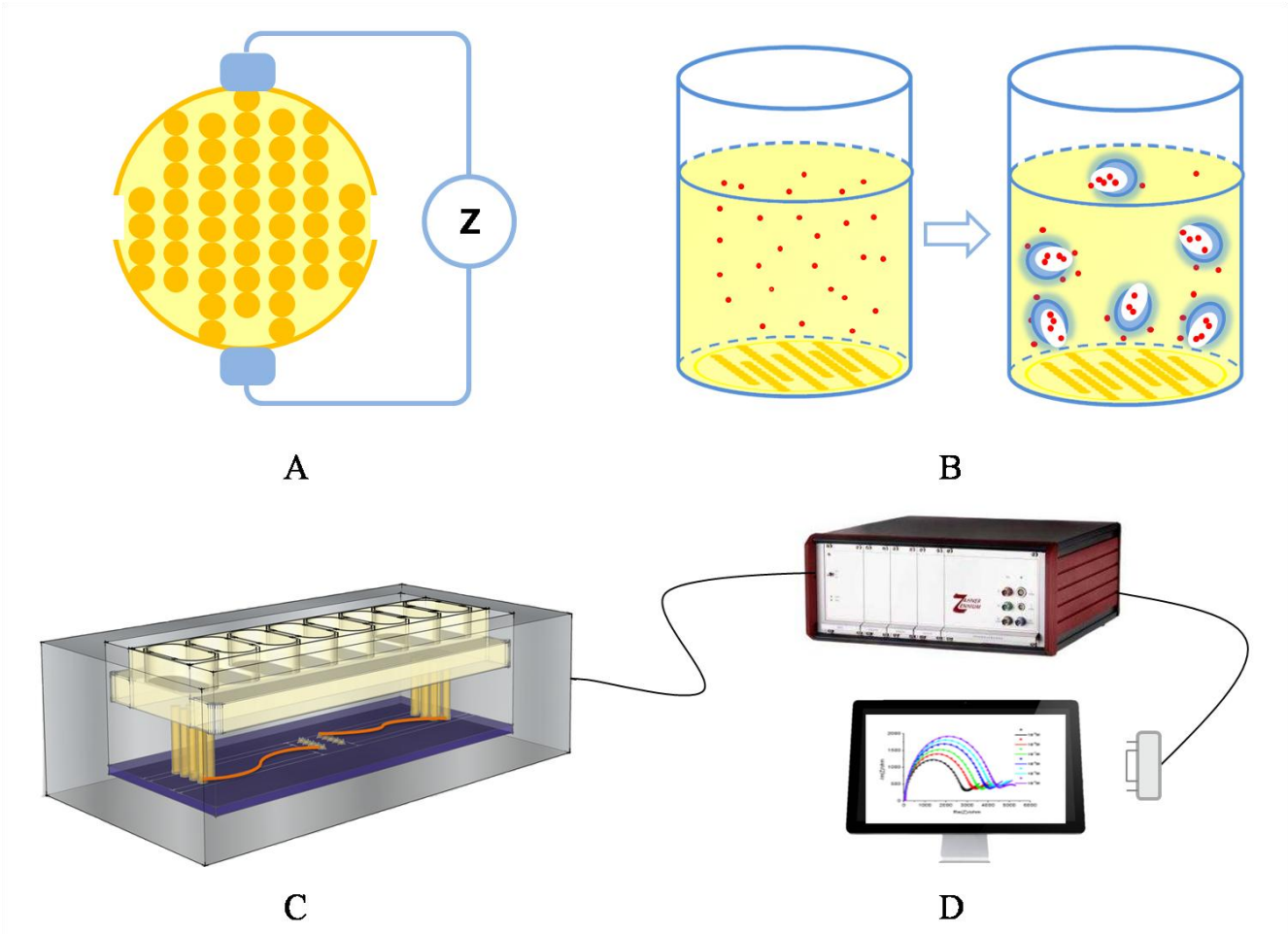

Figure 2. Biomimetic system for the impedance measurement. (A) Interdigitated electrodes in the bottom of the wells. (B) Schematic diagram of the ligands binding to the protein in the solution, the tiny red dots and the blue circles with a white cavity represented the ligands and the proteins, respectively. (C) Electrodes device and the circuit cavity of the biomimetic system. (D) Electrochemical workstation for impedance detecting.

The shape of electrodes was "circle-on-line" (Fig. 2A). There were 63 pairs of electrodes in each channel, and the longest pair of electrodes was 7.8 mm. The diameter of each circle on the electrodes was 90 μm, while the distance between two adjacent electrodes was 20 μm. The line part of the electrodes was 30 μm. The electrodes covered approximately 80% of the bottom areas of each well, which allowed for maximal sensitivity for the detection of the electrochemical reactions at the electrode interface. The schematic diagram of the ligand binding to the protein in the solution was used to demonstrate the binding process, especially stressed the pocket of the protein (Fig. 2B). The impedance measurements were performed using Zahner ZENNIUM electrochemical workstation (Zahner Elektrik, Germany). A special circuit cavity was designed for the electrode chip connecting with electrochemical workstation (Fig. 2C). The working electrode was connected to the test and sense probes on the electrochemical workstation by the circuit cavity, and the ground electrode was connected to the reference and counter probes of the workstation (Fig. 2D).

In order to verify whether the impedance sensing was also applicable to commonly used electrochemical platforms, controlled experiments were further conducted with a conventional three-electrode system. The three-electrode system consisted of working electrode (gold disk), counter electrode (platinum wire) and reference electrode (Ag/AgCl in saturated KCl). All of the electrodes were immersed in approximately half of the detected solution. The electrodes were connected with the test probes, counter and reference probes of the workstation, respectively.

2.5. Electrochemical measurements

The tested frequency was set from 0.1 Hz to 100 kHz with a 5 mV alternating voltage. After cleaning the interdigitated electrodes with ethanol and deionized water, isoamyl acetate were measured with 5 mM K_4 [Fe (CN) $_6$]/K_3[Fe(CN)$_6$] (1:1). After recording each concentration of isoamyl acetate, all of the solution was removed out of the plate well. Then, the electrodes were immersed in PBS for about 5 min to remove the residual ligands before the next test. Then, the mixture solution of Acer-ASP2 and isoamyl acetate of different concentrations (10^{-9} M to 10^{-4} M) was respectively recorded to get the dynamic binding process by the impedance sensing with the same detecting process. At each concentration, impedance spectroscopy was recorded for about 30 min. All of the experiments were carried out at room temperature (22 °C).

3. RESULTS AND DISCUSSION

3.1. Molecular docking and theoretical model

Based on molecular docking, the ligand-protein binding events were easy to be understood [19]. As illustrated in Fig. 3A, Acer-ASP2 consisted of six α-helices creating a predominantly internal binding pocket. According to the results of the molecular docking, the threonine side chain was likely to be a common hydrogen bond partner of this OBP. Oxygen atoms of most floral odors and pheromones can form hydrogen bond with Thr133, which is one of the most important amino acids in

the binding pocket according to molecular docking. As one of the pheromones, isoamyl acetate, which also has a chain structure, formed one hydrogen bond with Thr133. Butanedione acted as a negative control and formed one hydrogen bond with Tyr29. Based on the heuristic search algorithm that combines differential evolution with a cavity prediction algorithm, the fast and accurate identification of potential binding modes and poses could be obtained by the molecular docking. The results from molecular docking indicated the essence of biological reactions, which would be helpful for the exploration of the configuration and physiological function of this OBP.

Isoamyl acetate acted as chemical signals to transmit olfactory information and regulate behaviors of the honey bees. The concerted dynamic phenomenon occurred at the ligand entry site, which was likely related to the uptake mechanisms of the ligands [20]. A theoretical model was established to reveal the effect of sensing proteins in the charge transfer mechanisms induced by the ligand binding (Fig. 3B). The properties of solution were represented by Rs. R_P and C_P represented the resistance and capacitance of the protein, respectively. Meanwhile, R_L and C_L indicated the resistance and capacitance properties of the ligand in the protein cavity.

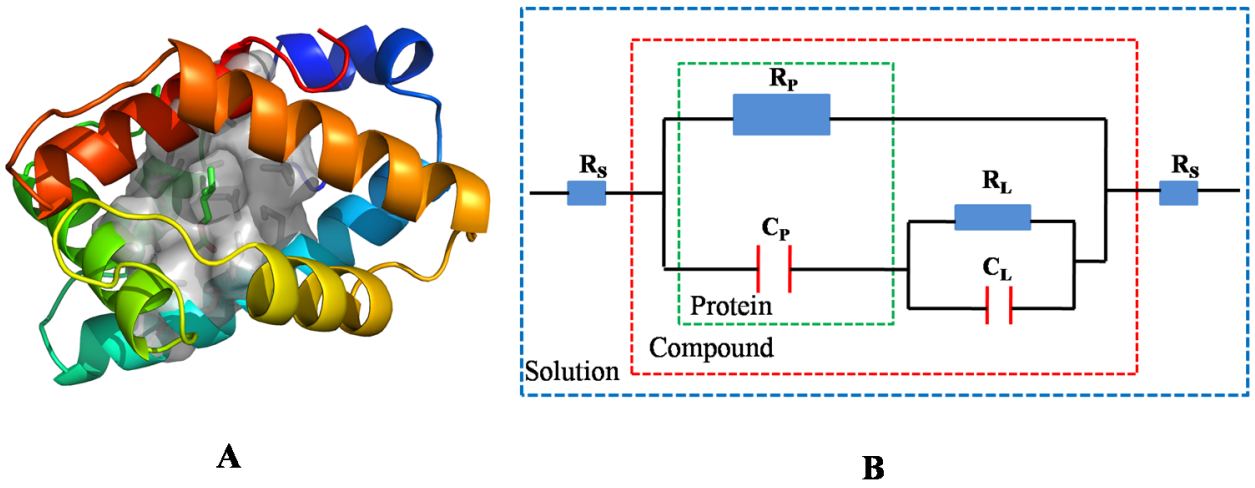

Figure 3. Structure and model of OBP. (A) Backbone structure of Acer-ASP2 with isoamyl acetate docked into its cavity. (B) A theoretical model of the solution and the OBP.

The impedance of Acer-ASP2 was dominated by the properties of amino acids, which influenced by the distance between each amino acid [21-22]. The independent RC parallel element (R_P and C_P) used to represent the properties of the protein. Little fluctuation was detected by the impedance system when the solution only contained protein or ligand. When protein and ligand formed the binding-compounds, the interactions had a prominent impact on the cavity of the protein. The additional R_L and C_L parallel to the resistance of protein (R_P) that led the reduction of the total resistance of the impedance system. However, if the ligand was not special for the protein, the resistance of the ligand was supposed to be in series with R_P. Therefore, the ligands binding to proteins could be detected by impedance sensing.

3.2. Biomimetic sensing of the odorants

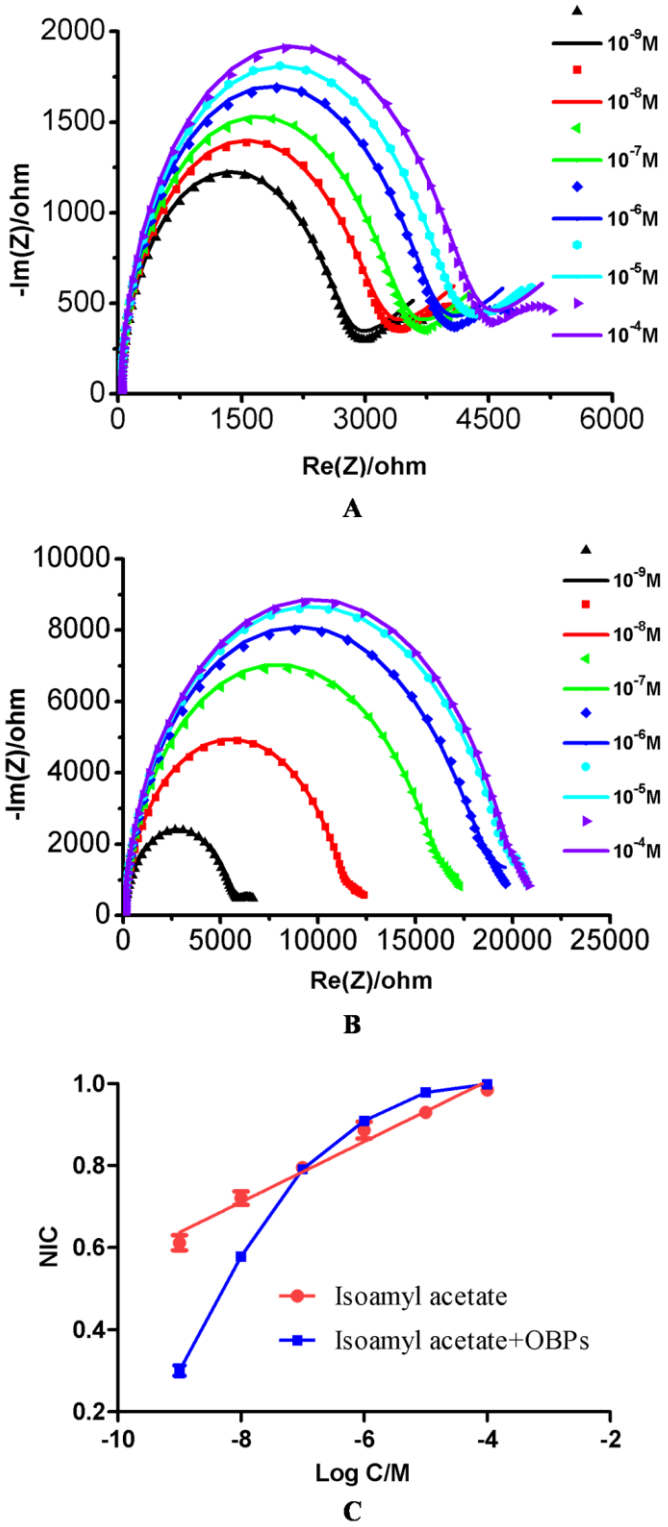

Figure 4. Impedance spectra of isoamyl acetate (A), and isoamyl acetate with the OBP (B). The symbols are the experimental data, and the lines represent the simulated spectra. The curve fitting for the logarithm of isoamyl acetate concentrations with and without the protein (C). The error bars represent the standard deviations of three repeated measurements.

For the situation of electrodes in contact with electrolyte, this complex system could be modeled to the Randles circuit. The circuit includes comprising the solution resistance Rs, the charge transfer resistance R_{ct}, the constant phase CPE and the Warburg impedance Z_w [23]. R_s and Z_w represent bulk properties of the electrolyte solution, respectively. Both CPE and R_{ct} depend on the dielectric and insulting features at the electrode/electrolyte interface [24]. They were affected by the property changes occurring at the interface. The ligand-protein binding events improved the efficiency of the mass transfer phenomenon, which reflected by R_{ct} in the impedance sensing. R_{ct} of the Randles circuit was chosen as the sensing parameter to characterize the protein-ligand interactions. Based on this circuit, we simulated the Nyquist plots recorded in the electrochemical experiments by Zview (Scribner Associates Inc., USA), to visualize and determine the changes of R_{ct}.

According to the experiments, the binding reactions between protein and odorants reached steady state within 30 min. So, the data at 30 min, can be used as the representative data of the finally stabilized. Fig. 4A and Fig. 4B displayed impedance spectra of isoamyl acetate without and with Acer-ASP2, respectively. By the combination of the molecular modeling with impedance detection, the insect OBP will provide a promising approach for chemical molecular sensing with their natural chemosensory abilities functionally preserved.

The diameter of the semicircle part of the Nyquist plot was equal to R_{ct} of the Randles circuit. The change of R_{ct} from the lowest concentration to the highest concentration was demonstrated through the normalized impedance (NIC) of R_{ct} (Fig. 4C). The NIC was described as NIC= R_a/R_b, where R_b represented R_{ct} of the highest concentration (10^{-4} M) while R_a represented R_{ct} of the other different concentrations. The NIC/LogC represented normalized impedance changes of per unit logarithmic concentration, which used to reflect the difference of variation of R_{ct} changed by the protein. Obviously, the higher concentration was, the larger R_{ct} obtained. Especially, the curve fitting for the logarithm of isoamyl acetate concentrations with protein became nonlinearity, which indicated the result of the binding process between proteins and ligands.

After simulating every spectrum, Impedance change (ΔR_{ct}) was chosen as the parameter to demonstrate the dynamic binding process of all concentrations. ΔR_{ct} was described as $\Delta R_{ct}=R_{cti}-R_{ct3}$. ΔR_{cti} represented the ΔR_{ct} of solution at i minute, i=3, 6, 9, 12, 15, 18, 21, 24, 27, 30. R_{ct3} represented R_{ct} of the first recording at the 3 minute. As shown in Fig. 5A, changes of R_{ct} of isoamyl acetate were recorded by interdigitated electrodes, which fluctuated within a small range. R_{ct} decreased apparently in the dynamic process of protein-ligand binding (Fig. 5B). In Fig. 5A, the R_{ct} gradually increased until a steady state was reached after 20 min. When the concentration went up to 10^{-4} M, the variability of the biosensor is slightly more obvious than that from any other lower concentrations and exhibited a slight declination after 10 min while fluctuated within a small range. In the presence of OBPs, the overall impedance changes were decreased. While, under the environment of higher concentrations (10^{-6} M, 10^{-5} M and 10^{-4} M), the changes of R_{ct} were obviously decreased than that in the concentrations of 10^{-9} M, 10^{-8} M and 10^{-7} M. The interactions between proteins and ligands in the binding site adding the additional R_L and C_L that paralleled to the resistance of proteins, resulting the decrease of the total resistance.

Acer-ASP2 performed excellent binding properties to isoamyl acetate with impedance sensing. Apparently, from 10^{-9} M to 10^{-6} M, the higher concentration was, the larger R_{ct} decreased. However,

the binding constants for OBPs binding to most ligands were micromole range [12, 25-26]. When the ligand concentration was higher than micromole range, the maximal variation of R_{ct} decreased. Compared with 10^{-6} M, isoamyl acetate at 10^{-5} M and 10^{-4} M had the similar binding affinity to OBPs. The impedance still had dynamic changes, but which suggested maybe there were excess ligands in the detecting solution. Although these excess ligands did not form the binding-compounds with proteins, the resistance of them still made contribution to the whole impedance of the biomimetic system, which made the dynamic changes of impedance decline.

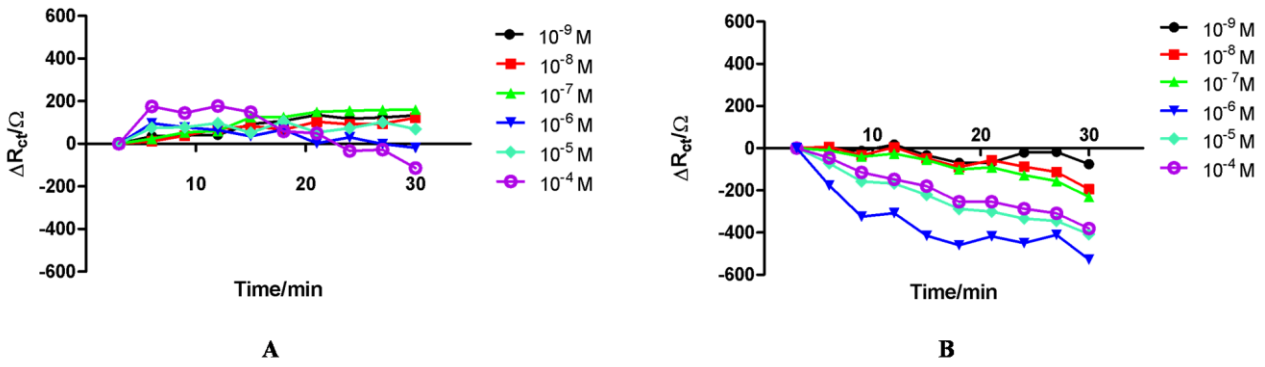

Figure 5. Dynamic impedance changes of isoamyl acetate (A), and isoamyl acetate with the OBP (B), recorded by the interdigitated electrodes.

Through impedance sensing, the dynamic binding of the OBPs and ligands could be detected, which was the results of conformation changes of OBPs that enhanced protein internal dynamics at the entry site. During the impedance sensing, the ligand binding and releasing could lead conformation of protein interconvert between a ligand-free open form and a ligand-bound closed form through a bending motion around the hinge [27]. When the ligands bonded into the cavity of OBPs forming binding-compounds, the ligand concentration in the solution decreased, which were reflected by the dynamic decreases of impedance.

3.3. Specificity of the sensor

As one of the widely used odorants in olfactory protein based biosensor [28], butanedione was taken as the negative ligand to show the specificity of OBPs. In our study, the impedance had little change for the stimulation of butanedione compared with isoamyl acetate (Fig. 6A). The impedance changes of all concentrations were comparatively stable. Moreover, the highest concentration also appeared to have a slight decrease within a small range after recording 10 min. The results indicated Acer-ASP2 showing a distinct response to butanedione because of the poor interactions. By the combination of the molecular modeling with impedance detection, the insect OBP will provide a promising approach for chemical sensing elements with their natural chemosensory abilities functionally preserved.

At the same time, as one of the commonly used proteins and the member of ligand-binding proteins family, BSA was treated as the negative protein to investigate the specificity of the OBPs to isoamyl acetate (Fig. 6B). According to the impedance sensing, there were no reduction of R_{ct}, which revealed BSA and isoamyl acetate did not form the binding-compound. The fluctuation of R_{ct} was similar with the fluctuation of R_{ct} of isoamyl acetate itself in the solution.

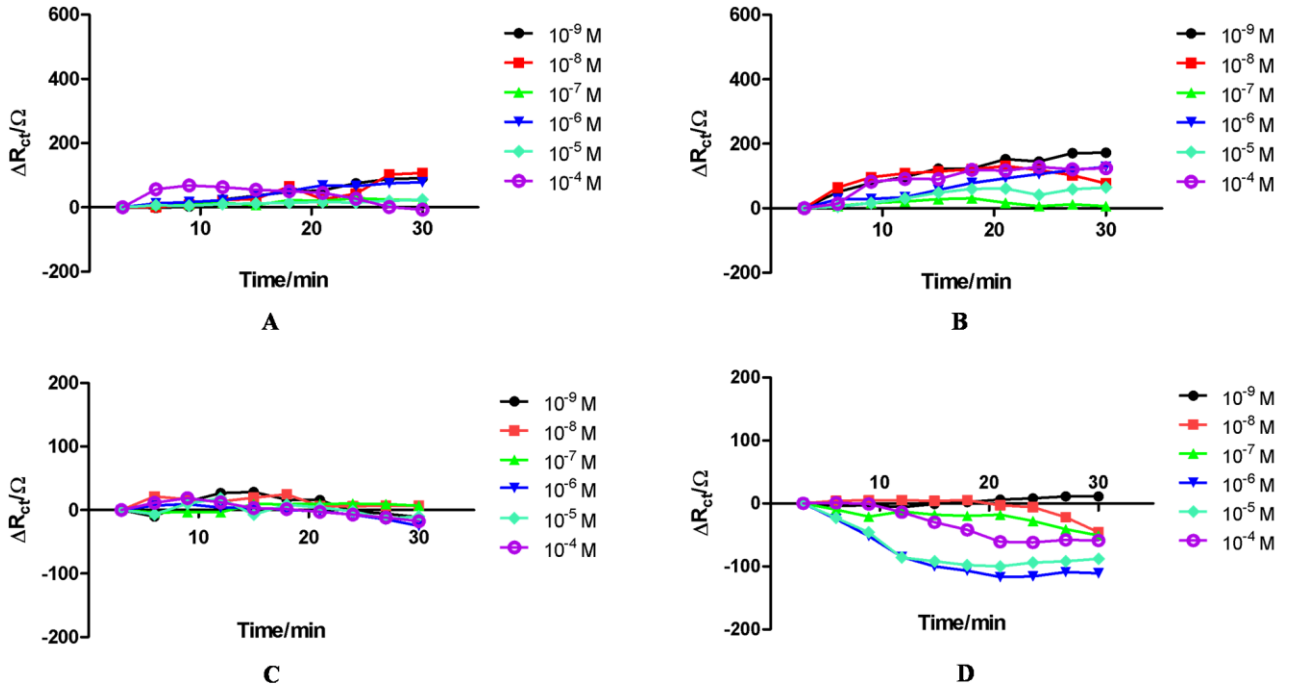

Figure 6. Specificity and sensitivity of the sensor. Dynamic impedance changes of the OBP with butanedione (A), and BSA with isoamyl acetate (B), recorded by the interdigitated electrodes. Dynamic impedance changes of isoamyl acetate (C), and isoamyl acetate with the OBP, recorded by the conventional three-electrode system (D)

The variation of R_{ct} of isoamyl acetate with OBPs recorded by conventional three-electrode system was shown in Fig. 6C and Fig. 6D. When monitoring the impedance changes of isoamyl acetate with and without OBPs, the tendency of impedance changes was similar to that recorded by interdigitated electrodes. However, in the presence of OBPs (Fig. 6D), the change range (within 150 Ω) was much smaller than that in Fig. 5B. Taking it as controlled sensor, isoamyl acetate showed similar affinities with the protein. It demonstrated that the impedance sensing was also applicable to commonly used electrochemical platforms of conventional three-electrode systems. However, it was obvious that interdigitated electrodes have higher sensitivity. The decrease of R_{ct} recorded by three-electrode system and interdigitated electrodes was within 150 Ω and 600 Ω, respectively.

Compared with conventional three-electrode system, interdigitated electrodes had a larger-area for solution contacting with electrodes, which allowed for a higher sensitivity for the detection of the electrochemical reactions at the electrode interface. What's more, interdigitated electrodes, which fabricated with microelectromechanical systems (MEMS), were easy to be designed for the high-

throughput detections in multchannel systems. Therefore, interdigitated electrodes provided a promising platform for detecting the dynamic binding events of OBPs.

3.4. Application analysis

The biomimetic olfactory sensors use biology elements as the sensing membrane, have many advantages over traditional techniques and can be used to detect various volatile compounds. The OBP-based biosensor provided a novel approach for electronic olfactory systems to detect odorants. Especially, the dynamic interactions between odorant and OBPs could be easily studied by the impedance sensing. It provided a promising approach to solve some practical problems. For example, one recent study revealed that bovine OBPs could be used to fabricate cartridges for removing the herbicide and similar compounds from waste water [29]. Another study utilized porcine OBPs to attenuate the unpleasant smells on the surface of textiles. [30]. Search for new solutions to prevent the development of unpleasant odors was of much interest for both the textiles and cosmetics industries. Use of the dynamic interactions between OBPs and corresponding ligands will be a new and exciting strategy for odor control from different materials. OBPs can be used to fabrics for masking the unpleasant smells like cigarette smoke. The capacity to capture the smell, the working time of absorbing odors and the kinds of odors that interacted with OBPs were foundation for these applications, which should be exactly calculated regarding the initial dynamic monitoring. All of these suggested that it's beneficial to study the dynamic interaction between odorants and OBPs.

At the same time, the biomimetic design was a label-free and ease of operating approach, compared with conventional techniques. Traditionally, odorants binding to OBPs were studied with fluorescence labelling, in which 1-aminoanthracene and N-phenyl-1-naphthylamine were widely used as probes for OBPs researches [31-32]. There are some drawbacks for applications, such as the procedures were time consuming, and cumbersome due to the labeling of the probes for binding events.

In our study, by directly detecting the OBPs and odorants with impedance sensing, dynamic binding properties could advance the progress in the understanding of biomimetic systems, which shows strong potentials for biotechnological applications. Through studying the sensitivity and selectivity of the sensor, the significant roles in the diversity of odors perception and in volatile molecules discrimination were proved. Thus, OBPs and other ligand-binding proteins will be used as promising recognition elements in the future biosensors. If needed, the approach could be applied to other proteins, which shows attractive potential for biotechnological applications.

4. CONCLUSIONS

A biomimetic system was designed to monitor and evaluate the dynamic process of ligand binding to protein by recording the electrochemical impedance spectroscopy. Based on molecular docking and the special cavity of OBPs, a theoretical model was established to discuss the correlations between the conformational changes of OBPs and impedance spectrum changes of the biosensor.

Compared with molecular docking, the impedance sensing reflected the global properties of binding events. The results suggested that the OBPs-based system could detect the odorants sensitively and selectively.

ACKNOWLEDGMENTS
This work was supported by the National Natural Science Foundation of China (Grant No. 81371643), the Zhejiang Provincial Natural Science Foundation of China (Grant No. LR13H180002; Y2110111).

Reference

1. T. C. Pearce, *BioSystems*., 41 (1997) 69.
2. S.H. Lee and T.H. Park, *Bio. Technol. Bioproc. E*., 15 (2010) 22.
3. R. Glatz and K. Bailey-Hill, *Prog. Neurobiol.*, 93 (2011) 270.
4. Q. Liu, H. Cai, Y. Xu, Y. Li, R. Li, and P. Wang, *Biosens. Bioelectron*., 22 (2006) 318.
5. Q. Liu, F. Zhang, N. Hu, H. Wang, K.J. Hsia, and P. Wang, *J. Bionic Eng.*, 9 (2012) 494.
6. L. Buck and R. Axel, *Cell*, 65 (1991) 175.
7. F.G. Vieira and J. Rozas, *Genome Biol. Evol*., 3 (2011) 476.
8. P. Pelosi, *Crit. Rev. Biochem. Mol. Biol*., 29 (1994) 199.
9. J. Fan, F. Francis, Y. Liu, J.L. Chen, and D.F. Cheng, *Genet. Mol. Res*., 10 (2011) 3056.
10. L. Kaiser, J. Graveland-Bikker, D. Steuerwald, M.Vanberghem, K. Herlihy, and S. Zhang, *Proc. Natl. Acad. Sci. U. S. A*., 105 (2008) 15726.
11. K. Corin, P. Baaske, D.B. Ravel, J. Song, E. Brown, X.Q. Wang et al., *PLoS ONE 6*, (2011) e25067.
12. S. Paolini, F. Tanfani, C. Fini, E. Bertoli, and P. Pelosi, *Biochim. Biophys. Acta*., 1431 (1999) 179.
13. L. Ban, A. Scaloni, C. D'Ambrosio, L. Zhang, Y. Yan, and P. Pelosi, *Cell Mol Life Sci*., 60 (2003) 390.
14. A. Schwaighofer, C. Kotlowski, C. Araman, N. Chu, R. Mastrogiacomo, C. Becker et al., *Eur. Biophys. J*., 43 (2014) 105.
15. R.A. Steinbrecht, *Ann. N. Y. Acad. Sci*., 855 (1998) 323.
16. H.J. Ko, S.H. Lee, E.H. Oh, and T.H. Park, *Bioprocess Biosyst. Eng*., 33 (2010) 55.
17. Y. Zhang, *BMC Bioinformatics*, *9* (2008) 40.
18. H. Li, L. Zhang, C. Ni, H. Shang, S.Zhuang, and J. Li, *Int. J. Biol. Macromol*., 56 (2013) 114.
19. R. Thomsen and M.H.Christensen, *J. Med. Chem*., 49 (2006) 3315.
20. E. Lescop, L. Briand, J.C. Pernollet, and E. Guittet, *Biochemistry*, 48 (2009) 2431.
21. E. Alfinito, J.F. Millithaler, C. Pennetta, and L.Reggiani, *Microelectr. J*., 41 (2010) 718.
22. E. Alfinito, C. Pennetta, and L. Reggiani, *Nanotechnol*., 19 (2008) 065202.
23. M.C. Rodriguez, A.N. Kawde, and J. Wang, *Chem. Commun.*, 34 (2005) 4267.
24. F. Lisdat and D. Schäfer, *Anal. Bioanal. Chem*., 391 (2008) 1555.
25. L. Brianda, J.C. Huet, V. Pereza, G. Lenoira, C.Nespoulousa, Y. Boucher et al., *FEBS Letters*, 476 (2000) 179.
26. P. Pelosi, M. Calvello, and L.Ban, *Chem. Senses*., 30 (2005) i291.
27. F.A. Quiocho and P.S. Ledvina, *Mol. Microbiol*., 20 (1996) 17.
28. J.H. Sung, H.J. Ko, and T.H. Park, *Biosens. Bioelectron*., 21 (2006) 1981.
29. F. Bianchi, G. Basini, S. Grolli, V. Conti, F. Bianchi, F. Grasselli et al., *Anal. Bioanal. Chem*., 405 (2013) 1067.
30. C. Silva, T. Matamá, N.G. Azoia, C. Mansilha, M.Casal, and A. Cavaco-Paulo, *Appl. Microbiol. Biotechnol*., 98 (2014) 3629.
31. S. Paolini, F. Tanfani, C. Fini, E. Bertoli, and P. Pelosi, *Biochim. Biophys. Acta*., 1431 (1999) 179.

32. P. Pelosi, R. Mastrogiacomo, I. Iovinella, E. Tuccori, and K.C. Persaud, *Appl. Microbiol. Biotechnol*., 98 (2014) 61.